Supporting Information

Xiao et al. 10.1073/pnas.1318899111

SI Materials and Methods

Protein Expression and Purification. A pET-23a plasmid containing the rat His_6-ERK2 sequence was transformed into *Escherichia coli* BL21(DE3) cells (1). A single colony was used to inoculate 1 mL of LB growth media containing 100 μg/mL carbenicillin and 34 μg/mL chloramphenicol, which was shaken overnight at 37 °C. Cells were resuspended in 25 mL of unlabeled M9 minimal medium in H_2O. At an OD_{600} of 0.8, the cells were spun down (1,600 × *g*, 10 min) and resuspended in 200 mL of M9 minimal medium with D-glucose-d_7 in D_2O, shaking at 37 °C until $OD_{600} \approx 0.6$. Cells were then spun down (1,600 × *g*, 10 min) and resuspended in 1 L of M9 minimal medium with 3 g/L D-glucose-d_7 and 1 g/L $^{15}NH_4Cl$ for U-[^{2}H,^{15}N] labeling, shaking at 37 °C. Precursors (α-keto-3-methyl-d_3-butyric acid-4-^{13}C and 2-ketobutyric acid-4-^{13}C) for Ile ($^{13}C^{\delta}H_3$), Leu ($^{13}C^{\delta}H_3$,$^{12}C^{\delta}D_3$), and Val ($^{13}C^{\gamma}H_3$,$^{12}C^{\gamma}D_3$) labeling were added to cells once the OD_{600} reached 0.8. After 1 h, the cells were induced with isopropyl-β-D-1-thiogalactopyranoside (2, 3) and shaken at 18 °C for 16 h, after which cells were centrifuged at 6,000 × *g* for 10 min. The cell pellets were resuspended in lysis buffer (50 mM NaH_2PO_4/Na_2HPO_4, pH 8.0, 300 mM NaCl, 0.1% β-mercaptoethanol, 5 mM imidazole, 1× Halt protease inhibitor, 1 mg/mL lysozyme, and 1 mM EDTA). The cell suspension was incubated at room temperature for 20 min and then sonicated and centrifuged at 24,000 × *g* for 45 min at 4 °C. The supernatant was collected as cell lysate. Proteins were purified from the cell lysate by Ni^{2+}-NTA affinity chromatography (Bio-Rad), PD-10 desalting (GE Healthcare), MonoQ FPLC (GE Healthcare), and Sephadex S200 size-exclusion chromatography (GE Healthcare) (4). Dual-phosphorylated (2P)-ERK2 was prepared from unphosphorylated (0P)-ERK2 after the MonoQ step, phosphorylated in vitro using constitutively active mutant MAP kinase kinase 1 (MKK-G7B: ΔN4/S218D/M219D/N221D/S222D) as described (5), and further purified by Sephadex S200 size-exclusion chromatography. The NMR samples of 0P-ERK2 and 2P-ERK2 were concentrated to 0.3–0.4 mM and exchanged into NMR buffer [50 mM Tris, pH 7.4, 150 mM NaCl, 5 mM $MgSO_4$, 0.1 mM EDTA, 5 mM DTT, 100% D_2O, and 2.5% (vol/vol) glycerol] for NMR experiments. Mutants of 0P-ERK2 I101A, L105A, M106E107GG, I124A, I131A, L154A, L155A, L161A, L198A, L235A, and I238A were created by site-directed mutagenesis of ERK2 using the QuikChange Mutagenesis Kit (Stratagene), confirmed by DNA sequencing, and purified in the same way as WT 0P-ERK2. The mutants were concentrated down to a final concentration of 0.1–0.4 mM in NMR buffer containing 5% (vol/vol) D_2O.

NMR Experiments for Assigning Residues. All of the NMR data used for making assignments were performed at 25 °C on a Varian VNMRS 800-MHz NMR spectrometer with a *z*-axis gradient cryoprobe and were processed using the software package NMRPipe (6). A 3D (^{13}C,^{13}C,^{1}H) HMCM[CG]CBCA ("out-and-back") experiment was performed on a 0.4 mM 0P-ERK2 sample that was ^{13}C-labeled and methyl-partially protonated on Ile, Leu, and Val side chains [Ile ($^{13}C^{\delta}H_3$), Leu ($^{13}C^{\delta}H_3$,$^{12}C^{\delta}D_3$), Val ($^{13}C^{\gamma}H_3$,$^{12}C^{\gamma}D_3$), and U-[^{15}N,^{13}C,^{2}H]]. This sample was expressed and purified as described above, except that a different set of precursors was used: 2-keto-3-(methyl-d_3)-1,2,3,4-$^{13}C_4$-3-d_1-butyrate and 2-keto-3,3-d_2-1,2,3,4-$^{13}C_4$-butyrate (7). The 3D (^{13}C,^{13}C,^{1}H) HMCM[CG]CBCA experiments were acquired with 64 and 42 complex points (4 and 10.5 ms, respectively) in the t_1 (C_{aliph}) and t_2 (C_m) dimensions and 1,024 complex points in acquisition period. ^{13}C decoupling was applied with WALTZ-16 during the 71-ms acquisition period (8). A 1.2-s delay period was used with 20 scans, leading to a total acquisition time of 83 h. Time-domain data in the ^{1}H dimension were apodized by a cosine window function and zero-filled before Fourier transformation. The indirect dimensions were also apodized by a cosine window function and zero-filled before Fourier transformation. Three-dimensional (^{13}C,^{13}C,^{1}H) heteronuclear multiple-quantum coherence (HMQC)-NOESY experiments were performed on Ile, Leu, and Val (ILV)-labeled samples of both 0P-ERK2 and 2P-ERK2 using a 350-ms mixing time. The experiments on 0P-ERK2 were acquired with 54 and 52 complex points (15.9 and 15.3 ms, respectively) in the t_1 (^{13}C) and t_2 (^{13}C) dimensions and 1,024 complex points in the acquisition period. GARP1 ^{13}C decoupling was applied during the 73-ms acquisition period (9). A 1.8-s delay period was used with eight scans, leading to a total acquisition time of 56 h. The NOESY experiments for 2P-ERK2 were essentially the same, except that 64 and 64 complex points were used (18.8 and 18.8 ms, respectively) in the t_1 (^{13}C) and t_2 (^{13}C) dimensions, resulting in a total acquisition time of 82 h. Time-domain data in the ^{1}H dimension were apodized by a squared cosine window function and zero-filled before Fourier transformation. The number of points in both indirect dimensions was doubled using forward–backward linear prediction (10). The indirect dimensions were then apodized by a cosine window function and zero-filled before Fourier transformation and baseline corrections were applied to both indirect dimensions.

A 2D (^{13}C,^{1}H) methyl transverse relaxation-optimized spectroscopy (TROSY) HMQC spectrum was collected on each 0P-ERK2 mutant (0.1–0.4 mM) with a total experimental time of 1–4 h. Parameters varied with protein concentration; for example, the spectrum of I124A at 0.2 mM was acquired with 160 complex points (29.5 ms) in the t_1 (^{13}C) dimension and 1,024 complex points in the acquisition period. WALTZ-16 ^{13}C decoupling was applied during the 85-ms acquisition period. A 1.5-s delay period was used with eight scans, leading to a total acquisition time of 1 h. The NMR data were processed as above.

Procedure for Assigning Residues. The procedure for making nonstereospecific resonance assignments of the ILV methyls ([$^{1}H_m$,$^{13}C_m$]) in 0P- or 2P-ERK2 primarily involved analysis of data from through-space and through-bond 3D NMR experiments in combination with the previously determined X-ray structures [Protein Data Bank (PDB) ID code 1ERK or 2ERK]. A series of mutants was then used to confirm the assignments.

The first step in the assignment procedure of 0P-ERK2 was to distinguish the Leu and Val methyls from each other using 3D (^{13}C,^{13}C,^{1}H) HMCM[CG]CBCA (out-and-back) experiments (7). Three resonances (Cγ, Cβ, Cα) were observed for each Leu methyl, whereas only two resonances (Cβ, Cα) were observed for each Val methyl (Fig. S1*A*). Methyl peaks from the same residue (L/V) shared the same Cα and Cβ chemical shifts, although this property was not sufficient to assign two methyl peaks to the same residue.

The next step was to identify spatially clustered ILV methyl groups from analysis of the 3D (^{13}C,^{13}C,^{1}H) HMQC-NOESY spectra (7), where the nuclear Overhauser effect (NOE) cross-peak intensities were qualitatively compared with distances between methyl protons in 0P-ERK2. Protons were added to PDB ID code 1ERK using the PDB Utility Servers (http://spin.niddk.nih.gov/bax/nmrserver) to calculate the shortest distances between the protons of two methyls. For example, a cluster of six Ile residues was identified from six Ile peaks that showed a set of

interconnecting NOEs in the 3D NOESY (Fig. S1*B*). Two Val peaks each showed NOEs to at least five Ile methyls in the Ile cluster (two of the Ile methyls had the same ^{13}C chemical shift; Fig. S1*B*). The fact that these two Val methyls did not show NOEs to each other, and had the same Cα and Cβ chemical shifts in the HMCM[CG]CBCA spectrum (Fig. S1*A*), strongly supports their assignments to the same residue. Next, the X-ray structure of 0P-ERK2 was screened for a large cluster of Ile methyls. The largest Ile cluster is composed of I54, I70, I84, I87, I101, and I345 (Fig. S1*C*), consistent with the six-Ile cluster found in the NOESY spectra. The surrounding Leu and Val methyls were used to make further assignments, where two Leu and one Val methyls were found close to this Ile cluster. Both methyls of V99 were close to most of the six Ile methyls, leading to direct or spin-diffusion NOEs to these Ile methyls. Thus, these two Val methyl peaks were assigned to V99. The next step in the assignment of the Ile methyls in the six-Ile cluster was measurement of the NOE cross-peak intensity for each of the Ile methyls to both methyls of V99. Two of the Ile methyls showed weak NOEs to V99, and both methyls showed NOEs to another Leu. Comparison of the NOE pattern and intensities with the X-ray structure led to tentative assignments for the other Ile methyls in this cluster as well as methyls on L67 and L74. A similar strategy was also used to assign methyls in other regions of the protein.

Once tentative assignments were made from the NOE data, 2D (^{13}C,^{1}H) methyl TROSY HMQC spectra of 10 ERK2 mutants, each substituting Ile, Leu, or Val with Ala, were used to adjust and confirm the tentative assignments. The absence of a peak in the spectra is used to help assign the resonance to a mutated residue (Fig. S1*D*). In some cases the mutation led to chemical shift changes in other methyl resonances, and therefore the HMQC spectra of the mutants by themselves did not generally provide unambiguous resonance assignments. The set of assignments of 0P-ERK2 was finalized by several iterations of these procedures, yielding 70 assignments of methyls to 62 residues. The assignments of 0P-ERK2 were then transferred to 2P-ERK2 and confirmed with 3D (^{13}C,^{13}C,^{1}H) HMQC-NOESY experiments on 2P-ERK2 (Fig. S1*E*), yielding assignments of 67 methyls to 60 residues.

Constant Time Carr–Purcell–Meiboom–Gill Relaxation Dispersion Experiments. Carr–Purcell–Meiboom–Gill (CPMG) relaxation dispersion experiments were performed on 0.3 mM 0P-ERK2 and 2P-ERK2 (the same samples that were used in NOESY experiments) at 25 °C using three field strengths (600, 800, and 900 MHz). The datasets of 800 and 900 MHz were collected on Varian VNMRS 800- and 900-MHz NMR spectrometers equipped with *z*-axis gradient cryoprobes. The 600-MHz datasets were collected on a Varian INOVA 600-MHz NMR spectrometer equipped with a room temperature probe. The experiment was arrayed with different delays (2τ) between ^{13}C refocusing pulses, with a total time of 20 ms (T_{relax}) (11). The experiment for 2P-ERK2 at 800 MHz was acquired with 12 different τ times corresponding to CPMG frequencies (ν_{CPMG}) ranging from 50 to 1,000 Hz. Several τ times were collected twice to estimate errors in the measurements. A set of 160 complex points in the t_1 (^{13}C) dimension and 1,024 complex points in the acquisition period was collected. A 2-s delay period was used with eight scans, leading to a total acquisition time of 21 h. Wideband Uniform Rate Excitation Smooth Truncation (WURST)-40 ^{13}C decoupling was applied during the 85-ms acquisition period (12). This experiment, with slightly different values of τ and numbers of complex points in the t_1 period, was repeated for 2P-ERK2 at 600 and 900 MHz, as well as for 0P-ERK2 at all three field strengths. Spectra were processed using NMRPipe (6), where the data for each τ were processed similar to a 2D HMQC spectrum described above. Peak intensities were measured using the program FuDA (http://pound.med.utoronto.ca/software). The effective decay rate ($R_{2,eff}$) was calculated by the equation (13) $R_{2,eff} = -1/T \ln[I(\nu_{CPMG})/I(0)]$, where $\nu_{CPMG} = 1/(4\tau)$, 2τ is the interval between successive 180° ^{13}C refocusing pulses, and $I(\nu_{CPMG})$ and $I(0)$ are the intensities of peaks recorded with and without the CPMG period, respectively. The CPMG dispersion profiles of 0P-, 2P-, and ME/GG-ERK2 were fit on a per-methyl basis to a two-state exchange process using the generalized Carver–Richards equation (11, 14), obtaining exchange rate constant ($k_{ex} = k_{AB} + k_{BA}$), populations of the two exchanging states (p_A, p_B), and ^{13}C chemical shift changes (in ppm) between states A and B ($|\Delta\delta_{CPMG}{}^{13}C|$, assuming $|\Delta\delta_{CPMG}{}^{1}H| = 0$). Fittings were performed using the program CATIA (http://pound.med.utoronto.ca/software). In addition, nonlinear least-squared fitting using the simplified, fast-exchange limit equation (14)

$$R_{2,eff} = R_{2,0} + \frac{p_A p_B \Delta\omega^2}{k_{ex}}\left(1 - \frac{2\ \tanh\left[\frac{k_{ex}\tau_{CP}}{2}\right]}{k_{ex}\tau_{CP}}\right)$$

was performed to estimate the term $p_A p_B \Delta\omega^2$ for methyls in 0P-ERK2 and ME/GG-ERK2. $R_{2,0}$ is the relaxation decay rate in the absence of exchange, τ_{CP} is the interval between successive 180° ^{13}C refocusing pulses (2τ), and Δω is the chemical shift difference in Hz between the two exchanging states A and B, which have populations of p_A and p_B, respectively.

1. Francis DM, et al. (2011) Resting and active states of the ERK2:HePTP complex. *J Am Chem Soc* 133(43):17138–17141.
2. Gardner KH, Kay LE (1997) Production and incorporation of N-15, C-13, H-2 (H-1-delta 1 methyl) isoleucine into proteins for multidimensional NMR studies. *J Am Chem Soc* 119(32):7599–7600.
3. Goto NK, Gardner KH, Mueller GA, Willis RC, Kay LE (1999) A robust and cost-effective method for the production of Val, Leu, Ile (delta 1) methyl-protonated ^{15}N-, ^{13}C-, ^{2}H-labeled proteins. *J Biomol NMR* 13(4):369–374.
4. Lee T, Hoofnagle AN, Resing KA, Ahn NG (2005) Hydrogen exchange solvent protection by an ATP analogue reveals conformational changes in ERK2 upon activation. *J Mol Biol* 353(3):600–612.
5. Shapiro PS, et al. (1998) Activation of the MKK/ERK pathway during somatic cell mitosis: Direct interactions of active ERK with kinetochores and regulation of the mitotic 3F3/2 phosphoantigen. *J Cell Biol* 142(6):1533–1545.
6. Delaglio F, et al. (1995) NMRPipe: A multidimensional spectral processing system based on UNIX pipes. *J Biomol NMR* 6(3):277–293.
7. Tugarinov V, Kay LE (2003) Ile, Leu, and Val methyl assignments of the 723-residue malate synthase G using a new labeling strategy and novel NMR methods. *J Am Chem Soc* 125(45):13868–13878.
8. Shaka AJ, Keeler J, Frenkiel T, Freeman R (1983) An improved sequence for broadband decoupling: WALTZ-16. *J Magn Reson* 52(2):335–338.
9. Shaka AJ, Lee CJ, Pines A (1988) Iterative schemes for bilinear operators; application to spin decoupling. *J Magn Reson* 77(2):274–293.
10. Zhu GA, Bax A (1992) 2-Dimensional linear prediction for signals truncated in both dimensions. *J Magn Reson* 98(1):192–199.
11. Korzhnev DM, Kloiber K, Kay LE (2004) Multiple-quantum relaxation dispersion NMR spectroscopy probing millisecond time-scale dynamics in proteins: Theory and application. *J Am Chem Soc* 126(23):7320–7329.
12. Kupce E, Freeman R (1995) Adiabatic Pulses for Wide-Band Inversion and Broad-Band Decoupling. *Journal of Magnetic Resonance Series A* 115(2):273–276.
13. Skrynnikov NR, Mulder FA, Hon B, Dahlquist FW, Kay LE (2001) Probing slow time scale dynamics at methyl-containing side chains in proteins by relaxation dispersion NMR measurements: Application to methionine residues in a cavity mutant of T4 lysozyme. *J Am Chem Soc* 123(19):4556–4566.
14. Palmer AG III (2004) NMR characterization of the dynamics of biomacromolecules. *Chem Rev* 104(8):3623–3640.

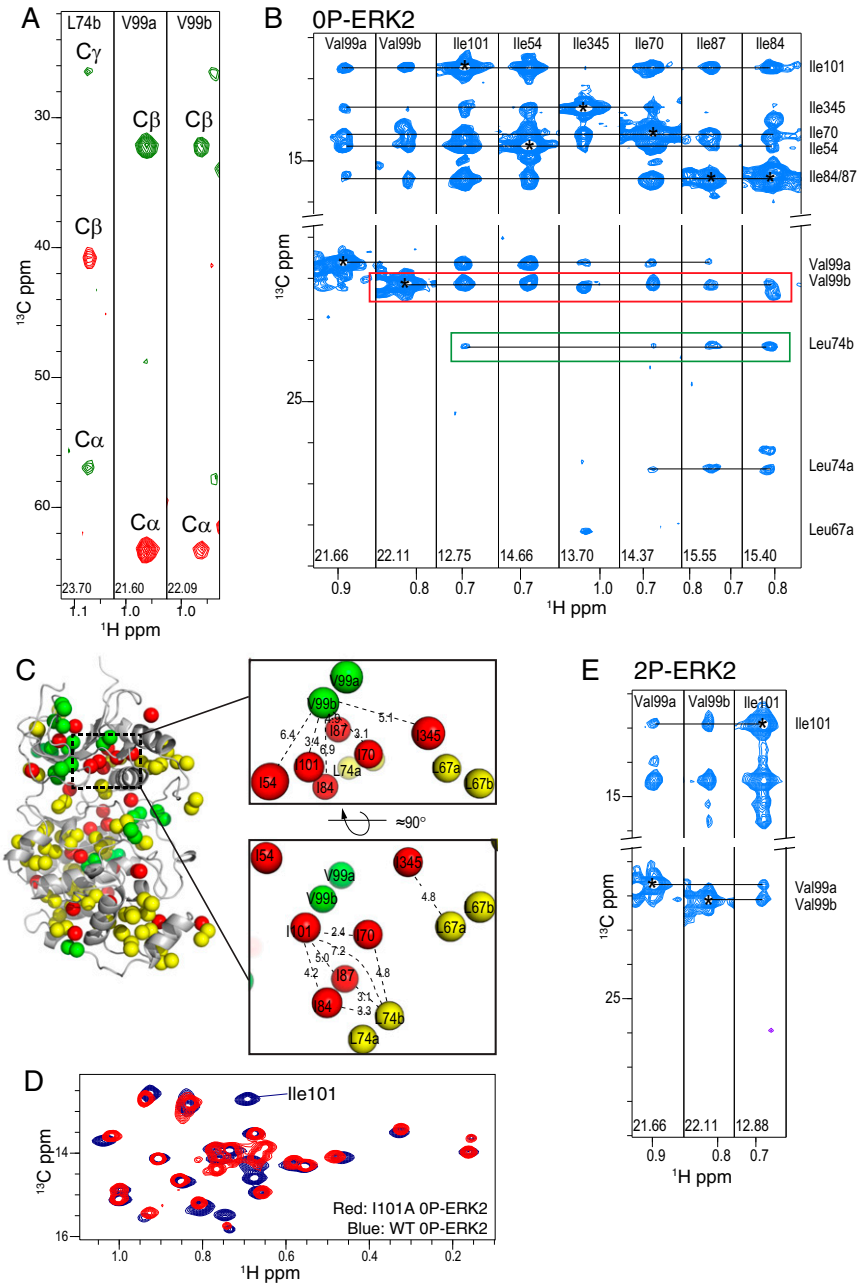

Fig. S1. Methods used for assigning ILV methyls in 0P- and 2P-ERK2. (*A*) Through-bond intraresidue (HMCM[CG]CBCA) experiments allowed distinction of Val from Leu methyls. Strip plots [^{1}H,^{13}C$_{aliph}$] of the 3D (^{13}C,^{13}C,^{1}H) HMCM[CG]CBCA spectra on an Ile (^{13}C$^{\delta}$H$_3$), Leu (^{13}C$^{\delta}$H$_3$,^{12}C$^{\delta}$D$_3$), Val (^{13}C$^{\gamma}$H$_3$,^{12}C$^{\gamma}$D$_3$), and U-[^{15}N,^{13}C,^{2}H] sample of 0P-ERK2 acquired at 800 MHz at 25 °C as described in *SI Materials and Methods*, showing examples of Leu (L74) and Val (V99) residues. The chemical shifts (ppm) for the ^{13}C$_{methyl}$ dimension are labeled at the bottom of each strip. The signs of the peaks alternate as magnetization is transferred along the carbon chain (i.e., Cα is 180° out of phase with Cβ, which is 180° out of phase with Cγ) as indicated by red (negative) and green (positive) contours. Val residues can be distinguished from Leu residues because the former only show two carbon resonances (Cα and Cβ), whereas the latter show three resonances (Cα, Cβ, and Cγ). Both methyl groups in V99 share the same Cα and Cβ chemical shifts, which helps assign them to the same residue. (*B*) Strip plots [^{1}H,^{13}C] from the 350-ms 3D (^{13}C,^{13}C,^{1}H) HMQC-NOESY spectrum of 0P-ERK2 illustrate that two Val methyl peaks (Val99a and Val99b) show NOEs to at least five Ile methyls (two of these Ile methyls have the same ^{13}C chemical shift). In addition, most of these Ile methyls show NOEs to each other. Three Leu methyl peaks, coming from at least two Leu residues, also show NOEs to a subset of the Ile methyls in this cluster. The chemical shifts (ppm) of the ^{13}C$_{methyl}$ dimension are labeled at the bottom of each strip, and the asterisks highlight methyl self-peaks. Cross-peaks that were used in the assignment were aligned with the self-peak as indicated by the horizontal lines. Cross-peaks for V99b and L74b are highlighted in red and green boxes, respectively. (*C*) X-ray structure of 0P-ERK2, where spheres represent methyls from Ile (red), Leu (yellow), and Val (green). The largest Ile cluster (I54, I70, I84, I87, I101, and I345) in the molecule is highlighted by the dashed box. The expansions illustrate this Ile cluster and adjacent Leu and Val methyls. Interresidue methyl proton–methyl proton distances are shown for V99b if a corresponding NOE cross-peak was observed in the NOESY spectrum in *B*. An ≈90° rotated view is shown to highlight L67 and L74, which are also close to the Ile cluster, and which provide additional information for assigning the Ile methyls in this cluster. L74b is relatively close to I84, I87, I70, and I101, and all these direct or spin diffusion-induced NOEs for L74b are observed in the NOESY spectrum in *B*. L67a is close to I345, and the corresponding NOE cross-peak is seen in *B*. (*D*) An overlay of the Ile methyl region of the 2D (^{13}C,^{1}H) methyl TROSY HMQC spectra of the wild-type (blue) and mutant I101A (red) sample of 0P-ERK2. Although multiple peaks showed clear chemical shift perturbations in this mutant, the absence of the I101 peak in the I101A 0P-ERK2 mutant was consistent with the assignment made from NOE data. (*E*) A similar pattern of NOE cross-peaks is seen in 2P-ERK2; strip plots are shown only for NOEs between V99 and I101.

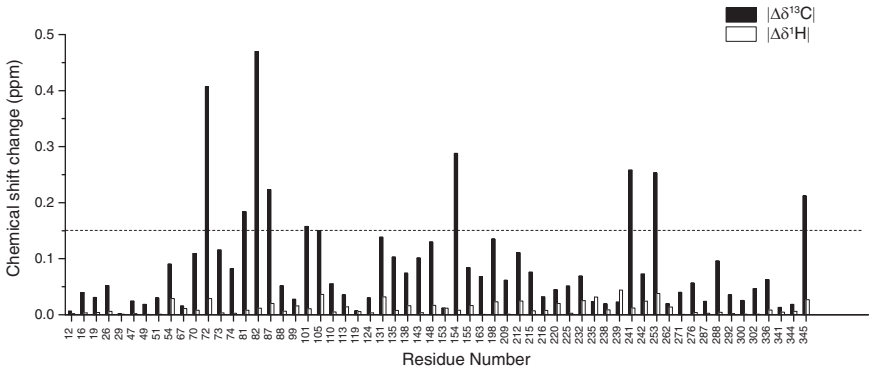

Fig. S2. Changes in chemical shifts and chemical environment between 0P-ERK2 and 2P-ERK2. Plot of the changes in carbon $|\Delta\delta^{13}C|$ (solid bars) and proton $|\Delta\delta^{1}H|$ (open bars) chemical shifts for the assigned methyl groups in 0P- and 2P-ERK2. The dashed line indicates a threshold of $|\Delta\delta| = 0.15$ ppm, which highlights methyls with the largest chemical shift changes induced by phosphorylation.

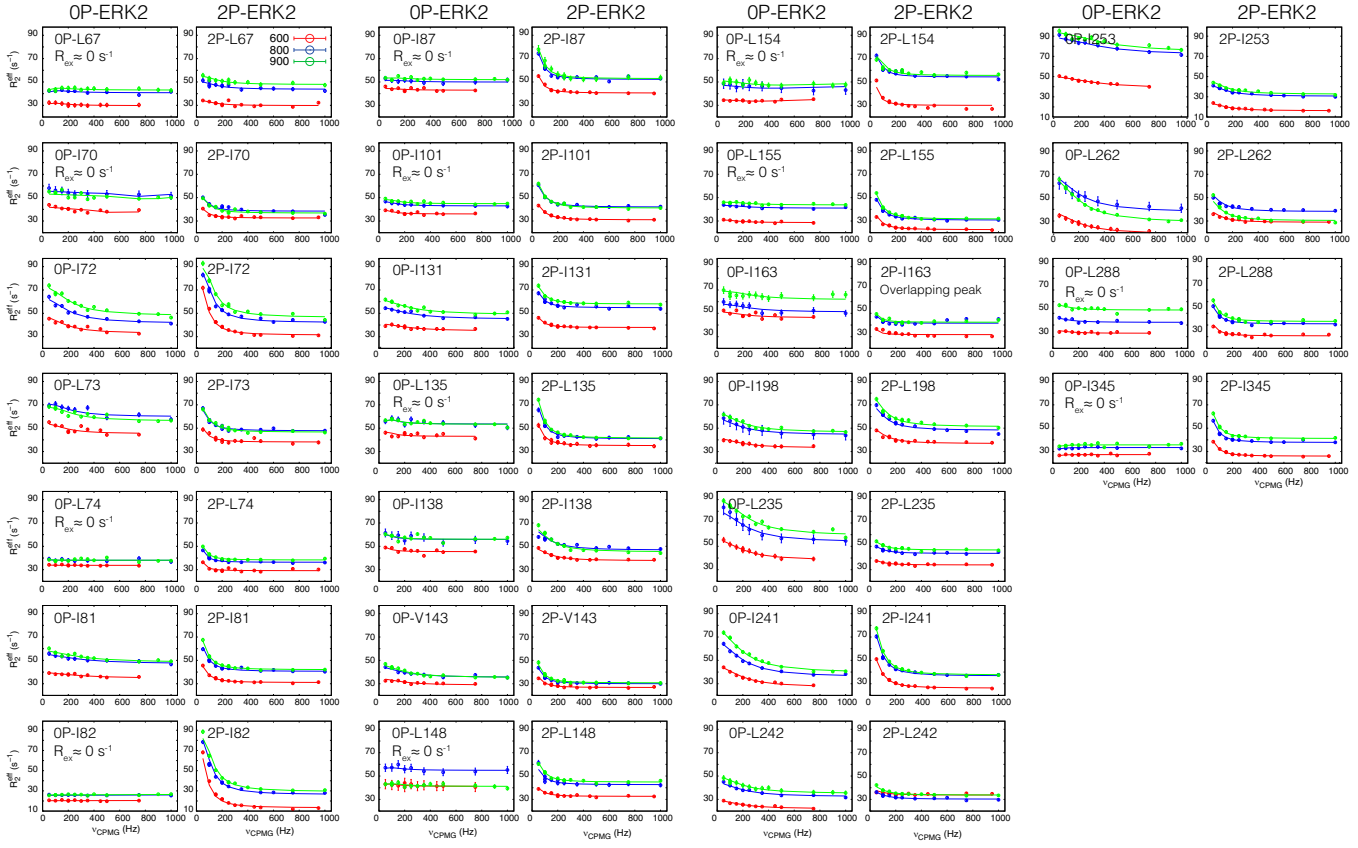

Fig. S3. CPMG relaxation dispersion curves for 0P- and 2P-ERK2. Relaxation dispersion curves at 25 °C and 900 (green), 800 (blue), and 600 (red) MHz are plotted for all residues that showed significant R_{ex} in either 0P-ERK2 (*Left*) or 2P-ERK2 (*Right*). Curves labeled "$R_{ex} \approx 0\ s^{-1}$" are residues where the dispersion was too small to confidently fit, meaning they had $R_{ex} < 4\ s^{-1}$. Lines show individual fits to the Carver–Richards equation, and the error bars were estimated from peak intensities of duplicate experiments.

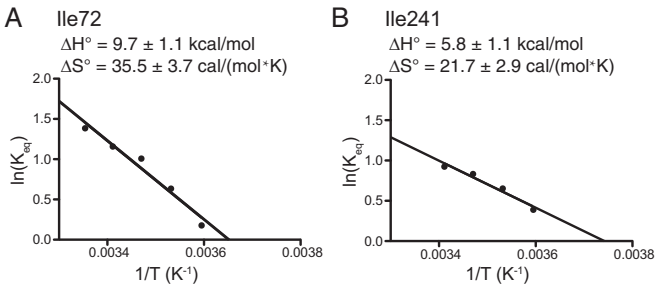

Fig. S4. Enthalpies and entropies estimated from 2D (^{13}C,^{1}H) HMQC spectra. van't Hoff plots for (*A*) I72 and (*B*) I241, where the K_{eq} values were estimated from the volumes of the two peaks that showed slow exchange for individual methyls in the HMQC spectra at different temperatures (Fig. 4).

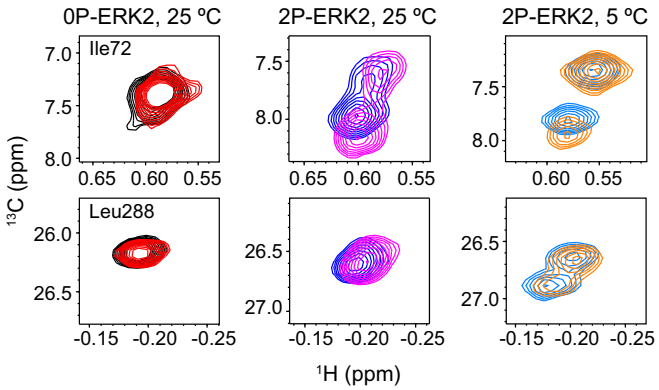

Fig. S5. Nucleotide binding does not affect populations of the two states in 0P- and 2P-ERK2. (*Left*) Two-dimensional (^{13}C,^{1}H) HMQC peaks of 0P-ERK2 at 25 °C with and without 1.35 mM adenosine-5′-(β,γ-imido)triphosphate (AMP-PNP) colored in red and black, respectively. (*Center*) 2P-ERK2 at 25 °C with and without 1.15 mM AMP-PNP, colored in magenta and blue, respectively. (*Right*) 2P-ERK2 at 5 °C with and without 1.15 mM AMP-PNP, colored in orange and sky blue, respectively.

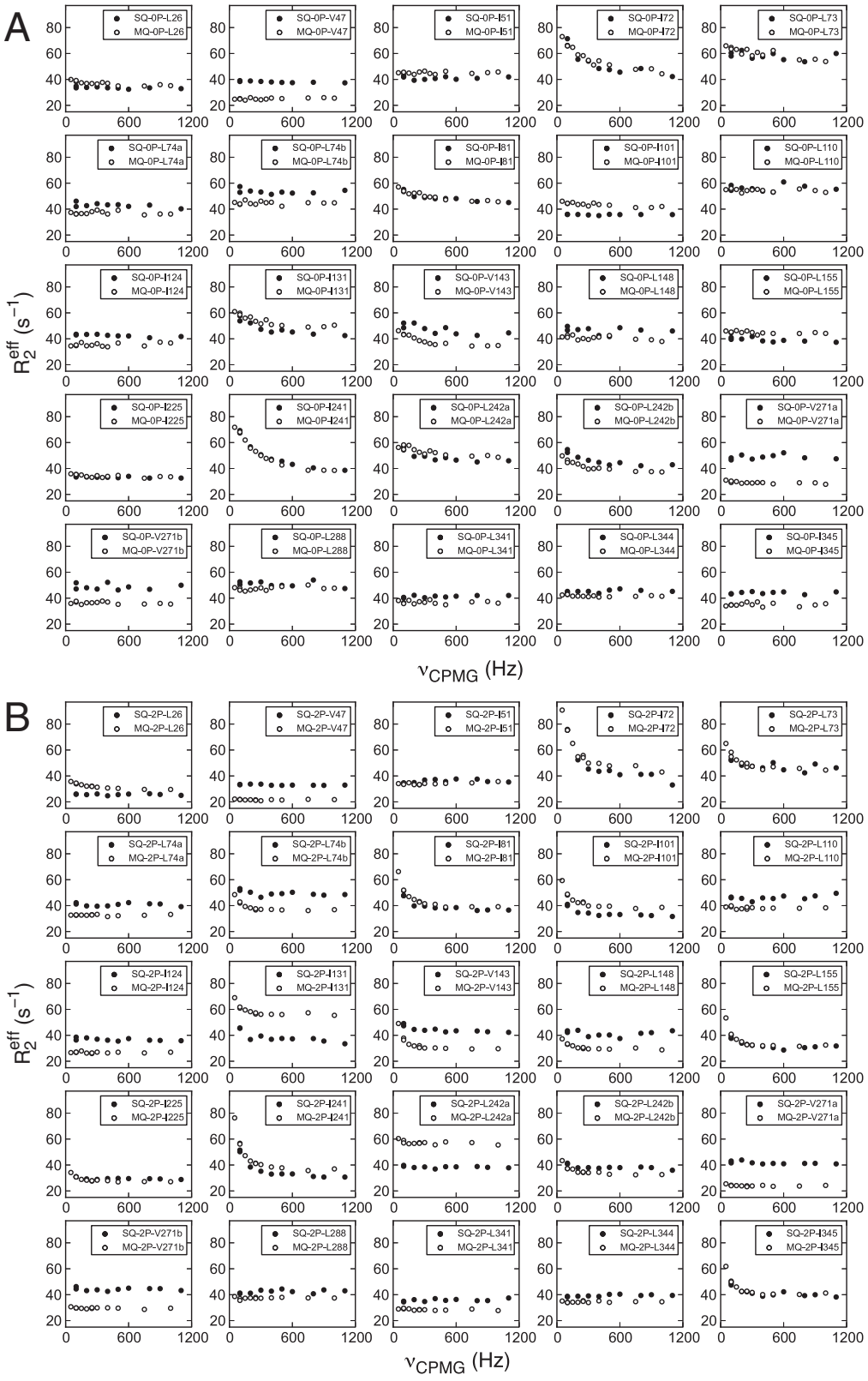

Fig. S6. Single-quantum CPMG experiments show dispersion profiles similar to multiple-quantum CPMG experiments. CPMG dispersion curves were comparable between 2D (^{13}C,^{1}H) single-quantum CPMG experiments (SQ; closed circles) and 2D (^{13}C,^{1}H) multiple-quantum CPMG experiments (MQ; open circles), for (*A*) 0P-ERK2 and (*B*) 2P-ERK2. Each set of experiments was carried out at 900 MHz and 25 °C.

Table S1. Exchange parameters for methyl groups in 0P-ERK2, fitted individually*

Residue	Parameters			
	k_{ex}, s^{-1}†	$R_{ex}(800)$, s^{-1}‡	$p_A p_B(\Delta\omega^{13}C)^2$, s^{-2}§	χ^2/DF¶
Kinase core				
Ile72	1,400 ± 400	23	32,000 ± 5,000	2.2
Leu73	900 ± 700	12	16,000 ± 8,000	3.2
Ile81	2,000 ± 600	9	26,000 ± 9,000	0.8
Ile131	1,700 ± 700	9	26,000 ± 10,000	0.9
Ile138‖	N.D.	7	N.D.	N.D.
Val143	1,100 ± 600	9	11,000 ± 4,000	1.0
Ile163‖	N.D.	10	N.D.	N.D.
Ile241	1,100 ± 200	26	40,000 ± 2,000	1.0
Leu242	1,500 ± 300	13	19,000 ± 3,000	0.8
MAP kinase insert				
Leu198	1,300 ± 300	15	10,000 ± 2,000	0.4
Leu235	1,200 ± 200	29	45,000 ± 3,000	1.0
Ile253	2,200 ± 300	20	62,000 ± 15,000	0.9
Leu262	1,400 ± 300	22	34,000 ± 3,000	0.5

*These parameters were all obtained from MQ CPMG dispersion data collected at 25 °C.

†The k_{ex} values were obtained by fitting CPMG dispersion data collected at 600, 800, and 900 MHz to a two-state exchange process using the Carver–Richards equation on a per-methyl basis. The errors were estimated from fits using the CATIA program, and may be underestimated if the data are not well-described by a two-state exchange process (*Materials and Methods*).

‡$R_{ex}(800)$ was estimated using the equation $R_{ex} = R_{2,eff}(50\ Hz) - R_{2,eff}(1{,}000\ Hz)$ from 800-MHz CPMG dispersion data.

§This term was estimated assuming a two-state exchange model under fast-exchange limit using 800-MHz CPMG dispersion data (*Materials and Methods*).

¶χ^2/DF (reduced χ^2) describes the quality of the fit for the experimental data. DF is the degrees of freedom and was calculated by DF = (number of experimental data points – number of parameters – 1) for each methyl in the dataset.

‖Individual fits were not determined (N.D.) due to large errors, but the R_{ex} could still be estimated.

Table S2. Exchange parameters for methyl groups in 2P-ERK2, fitted individually*

Residue	Parameters					
	k_{ex}, s^{-1}†	p_B, %†	$\lvert\Delta\delta_{CPMG}{}^{13}C\rvert$, ppm†	$R_{ex}(800)$, s^{-1}‡	χ^2/DF§	$\lvert\Delta\delta_{CPMG}{}^{13}C_{global}\rvert$, ppm¶
Kinase core						
Leu67	550 ± 400	2 ± 1	0.6 ± 0.3	9	2.3	0.1 ± 0.01
Ile70	210 ± 100	8 ± 2	0.4 ± 0.09	15	2.3	0.2 ± 0.01
Ile72	150 ± 60	28 ± 8	0.7 ± 0.07	40	2.7	0.6 ± 0.02
Leu73	230 ± 80	13 ± 2	0.4 ± 0.06	19	1.3	0.3 ± 0.01
Leu74‖	N.D.	N.D.	N.D.	10	N.D.	0.2 ± 0.01
Ile81	110 ± 60	17 ± 6	0.5 ± 0.09	19	0.7	0.3 ± 0.01
Ile82	140 ± 60	35 ± 12	0.7 ± 0.08	50	8.3	0.6 ± 0.02
Ile87	200 ± 90	19 ± 4	0.4 ± 0.1	22	0.9	0.3 ± 0.01
Ile101	220 ± 50	13 ± 2	0.4 ± 0.05	18	0.6	0.3 ± 0.01
Ile131	190 ± 50	11 ± 2	0.4 ± 0.05	13	0.5	0.2 ± 0.01
Leu135	180 ± 90	18 ± 3	0.4 ± 0.1	24	0.6	0.3 ± 0.01
Ile138	110 ± 90	8 ± 6	0.9 ± 0.1	10	2.1	0.3 ± 0.01
Val143	190 ± 50	16 ± 6	0.3 ± 0.06	14	0.8	0.2 ± 0.01
Leu148	290 ± 60	16 ± 6	0.3 ± 0.04	19	1.1	0.2 ± 0.01
Ile154‖	N.D.	N.D.	N.D.	20	N.D.	0.3 ± 0.01
Leu155	290 ± 50	13 ± 3	0.4 ± 0.05	17	1.6	0.3 ± 0.01
Leu241	160 ± 50	21 ± 3	0.5 ± 0.06	33	0.8	0.4 ± 0.01
Leu288	260 ± 220	15 ± 18	0.3 ± 0.3	16	1.7	0.2 ± 0.01
Ile345	380 ± 30	20 ± 20	0.1 ± 0.01	19	0.6	0.3 ± 0.01
Global fitting	300 ± 10	80 ± 0.6	—	—	1.0	See above
MAP kinase insert						
Leu198	750 ± 340	20 ± 100	0.3 ± 0.7	25	2.0	—
Leu235‖	N.D.	N.D.	N.D.	5	N.D.	—
Ile253	750 ± 130	5 ± 3	0.5 ± 0.2	11	0.8	—
Leu262	640 ± 80	60 ± 70	0.1 ± 0.04	11	0.8	—

*These parameters were all obtained from MQ CPMG dispersion data collected at 25 °C.

†These parameters were all obtained by fitting CPMG dispersion data collected at 600, 800, and 900 MHz to a two-state exchange process using the Carver–Richards equation on a per-methyl basis. The errors were estimated from fits using the CATIA program, and may be underestimated if the data are not well-described by a two-state exchange process (*Materials and Methods*).

‡$R_{ex}(800)$ was estimated using the equation $R_{ex} = R_{2,eff}(50\ Hz) - R_{2,eff}(1{,}000\ Hz)$ from 800-MHz CPMG dispersion data.

§χ^2/DF (reduced χ^2) describes the quality of the fit for the experimental data. DF is the degrees of freedom and was calculated by DF = (number of experimental data points − number of parameters − 1) for each methyl in the dataset.

¶$\lvert\Delta\delta_{CPMG}{}^{13}C_{global}\rvert$ is obtained by a global fitting of the methyls in the kinase core that showed $R_{ex}(800) > 4\ s^{-1}$ using CATIA.

‖Individual fits were not determined due to large errors, but the R_{ex} could still be estimated.

Table S3. Exchange parameters for methyl groups in ME/GG-ERK2, fitted individually*

Residue	Parameters				
	k_{ex}, s^{-1}†	R_{ex}(800), s^{-1}‡	$p_A p_B(\Delta\omega^{13}C)^2$, s^{-2}§	χ^2/DF¶	$\lvert\Delta\delta_{CPMG}{}^{13}C_{global}\rvert$, ppm‖
Kinase core					
Ile54	900 ± 500	9	7,000 ± 1,000	1.2	0.4 ± 0.05
Ile72	1,100 ± 800	13	28,000 ± 12,000	0.9	1 ± 0.1
Ile82	500 ± 100	6	4,400 ± 800	0.3	0.3 ± 0.04
Ile84**	N.D.	7	N.D.	N.D.	0.3 ± 0.04
Val99**	N.D.	6	N.D.	N.D.	0.3 ± 0.04
Ile101	1,000 ± 300	8	10,000 ± 2,000	0.9	0.5 ± 0.05
Leu105**	N.D.	4	N.D.	N.D.	
Leu110	800 ± 300	13	31,000 ± 10,000	0.4	1.1 ± 0.1
Ile113**	N.D.	4	N.D.	N.D.	
Ile124	200 ± 170	4	3,400 ± 800	0.2	
Ile131	1,700 ± 700	12	50,000 ± 45,000	4	0.9 ± 0.1
Leu135**	N.D.	6	N.D.	N.D.	0.5 ± 0.04
Ile138**	N.D.	7	N.D.	N.D.	0.4 ± 0.04
Val143	500 ± 200	8	7,500 ± 3,200	1.0	0.3 ± 0.05
Leu148**	N.D.	4	N.D.	N.D.	
Leu154	1,400 ± 800	8	16,000 ± 3,000	0.9	0.7 ± 0.05
Leu155	1,900 ± 600	8	31,000 ± 15,000	0.8	0.4 ± 0.04
Leu209	200 ± 100	6	3,600 ± 400	2.7	0.3 ± 0.04
Leu225	400 ± 100	6	4,700 ± 700	0.2	0.3 ± 0.04
Ile241	700 ± 200	17	26,000 ± 2,000	0.1	0.9 ± 0.1
Leu242**	N.D.	8	N.D.	N.D.	0.4 ± 0.03
Global fitting	500 ± 60	—	p_B = 3 ± 0.2%	1.0	See above
MAP kinase insert					
Leu198	1,200 ± 300	11	21,000 ± 3,000	0.9	—
Leu235	1,400 ± 800	20	34,000 ± 4,000	1.4	—
Ile253	1,600 ± 1,200	11	36,000 ± 18,000	0.6	—
Leu262	1,300 ± 600	28	95,000 ± 25,000	4.6	—

*These parameters were all obtained from MQ CPMG dispersion data collected at 25 °C.

†These parameters were all obtained by fitting CPMG dispersion data collected at 600, 800, and 900 MHz to a two-state exchange process using the Carver–Richards equation on a per-methyl basis. The errors were estimated from fits using the CATIA program, and may be underestimated if the data are not well-described by a two-state exchange process (*Materials and Methods*).

‡R_{ex}(800) was estimated using the equation $R_{ex} = R_{2,eff}$(50 Hz) – $R_{2,eff}$(1,000 Hz) from 800-MHz CPMG dispersion data.

§This term was estimated assuming a two-state exchange model under fast-exchange limit using 800-MHz CPMG dispersion data (*Materials and Methods*).

¶χ^2/DF (reduced χ^2) describes the quality of the fit for the experimental data. DF is the degrees of freedom and was calculated by DF = (number of experimental data points – number of parameters – 1) for each methyl in the dataset.

‖$\lvert\Delta\delta_{CPMG}{}^{13}C_{global}\rvert$ is obtained by a global fitting of the methyls in the kinase core that showed $R_{ex}(800) > 4\ s^{-1}$ using CATIA.

**Individual fits were not determined due to large errors, but the R_{ex} could still be estimated.